Journal of Physics and Chemistry of Solids 87 (2015) 158–162

Contents lists available at ScienceDirect

Journal of Physics and Chemistry of Solids

journal homepage: www.elsevier.com/locate/jpcs

Optical bistability in gold nano-colloid due to thermal lensing effect

E. Koushki [a,b], H. Akherat Doost [a], M.H. Majles Ara [a,*]

[a] Photonics Laboratory, Physics Faculty, Kharazmi University, Mofateh 49, Tehran, Iran
[b] Physics Department, Hakim Sabzevari University, Sabzevar, Iran

A R T I C L E I N F O

Article history:
Received 19 February 2015
Received in revised form
25 July 2015
Accepted 7 August 2015
Available online 8 August 2015

Keywords:
Non-crystalline materials
Optical materials
Optical properties
Thermal expansion

A B S T R A C T

In this study, experimental results are concerning "the optical bistability due to thermal lensing effect", in colloidal solution of gold nanoparticles (Au Nps) which has been studied under CW laser illuminations. Two different CW laser beams (He–Ne and Nd-Yag) were used to interact with a vertical Fabry–Perot interferometer, containing colloid of the Au Nps. Hysteretic loops have been observed with regard to optical bistability and the results were fitted with theoretical curves. The radiated power to the resonator was elevated up to 50 mW for both the laser beams with the same spot size. Also, new method was defined to precise evaluation of the theoretical hysteretic loop which is describing the relation between nonlinear refractive index and the beam intensity inside the resonator. This dependency is due to thermal lensing effect and numerical simulations of this effect were also performed, in order to better understanding of it.

1. Introduction

Bistable devices are important in digital electronics and also are the basic building blocks of computer systems. They are used as switchers, logic gates and memory elements [1,2].

On the other hand, metals and semiconductor nanoparticles were great chance for researchers due to their unique optical properties [3–5]. Various nanomaterials based on metals, semiconductors, and dielectrics have been synthesized by different techniques and their unique electrical and optical properties are comprehensively studied by researchers. Nanoparticles have also interesting nonlinear optical properties with regard to the long path of surface plasmonic electrons or special size dependent to the bang gap. Optical nonlinearity in some nanoparticles has been studied by using various methods in many articles [6–8]. Optical properties of gold nanoparticles (Au Nps) have widely been studied in these years [9–12]. In this work, Au Nps are used as optical bistable devices in low power laser irradiations.

Certain nonlinear optical systems can possess two output states for a given input state. Two features are required to make a bistable device: optical nonlinearity and feedback. An optical bistable device is consists of a nonlinear optical element which output beam is applied in a feedback system to control the transmission of light through the element itself. Combination of the beam and its feedback will cause the curves of output intensity (I_3) versus input one (I_1) become a steep S-shape. The curves of experimental results do not follow the S-shape curve. They contain a hysteretic loop that could include S-shape deviation. As the input intensity exceeds from the critical points of the hysteretic loop, the output one jumps into another magnitudes on the other trace of the loop [12–14].

The main parameters are the transmittance of the mirrors and the optical indices of the material [12–14]. In low intensity irradiations, the main portion of optical nonlinearity is due to thermal lensing effect [15,16]. Linear and nonlinear absorption heats up the sample locally and thermal expansion leads to decrease the refractive index. Therefore, the refractive index depends on the intensity and could be considered as a nonlinear quantity. This dependency is a function of many parameters such as the beam properties and the sample parameters. Considering these parameters, simulation of thermal lensing effect for Au Nps would be possible.

2. Theory

A Fabry–Perot resonator is schematically illustrated in Fig. 1. The distance between two mirrors has been filled with a nonlinear sample. Here A_1 denotes the field amplitude of the incident wave, A_1' denotes the reflected wave, A_2 and A_2' denotes the amplitudes of the forward- and backward-going waves within the interferometer, and A_3 denotes the amplitude of the transmitted wave. The mirrors are assuming to be lossless, with amplitude reflectance ρ_1 and ρ_2, respectively and transmittance τ_1 and τ_2 that

* Correspondence to: Photonics Laboratory, Physics Department, Kharazmi University, 49 Moffateh Avenue, P.O. Box 1571914911, Tehran, Iran.
E-mail address: majlesara@gmail.com (M.H. Majles Ara).

http://dx.doi.org/10.1016/j.jpcs.2015.08.003

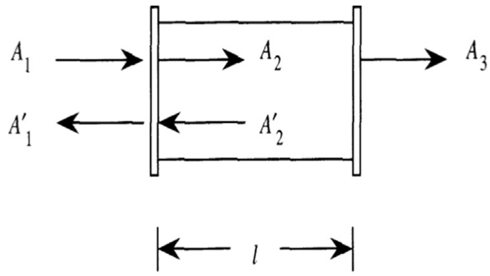

Fig. 1. Schematic description of a Fabry–Perot resonator.

are related to the reflectance R and transmittance T through [13,17]

$$R_i = |\rho_i|^2 \; T_i = |\tau_i|^2 \qquad i = 1, 2 \tag{1}$$

with

$$R + T = 1 \tag{2}$$

The incident and internal fields have been related to each other through boundary conditions of the form [13,17]

$$A_2 = \tau_1 A_1 + \rho_1 A'_2 \tag{3}$$

$$A'_2 = \rho_2 A_2 \exp(2ikl - \alpha_t l) \tag{4}$$

In these equations, we assume that the field amplitudes are measured at the inner surface of the left-hand mirror. The propagation constant $k = \frac{\omega}{c}(n_0 + n_2 I_2)$ and the intensity absorption coefficient $\alpha_t = \alpha + \beta I_2$ are taking to be real and containing both the linear and nonlinear contributions (I_2 is the intensity of the field A_2 inside the cavity). In writing Eq. (4) in the form shown, we have implicitly made the *mean-field approximation*, which we have assumed that, the quantities k and α_t are spatially invariant. Eqs. (3) and (4) can be algebraically solved by eliminating A'_2 to obtain [13,17]:

$$A_2 = \frac{\tau_1 A_1}{1 - \rho_1 \rho_2 \exp(2ikl - \alpha_t l)} \tag{5}$$

We also have:

$$A_3 = \tau_2 A_2 \exp\left(ikl - \frac{\alpha_t l}{2}\right) \tag{6}$$

Eqs. (5) and (6) describe the properties of a Fabry–Perot interferometer [13]. We remember that the intensity of the fields is [13,17]:

$$I_i = \frac{n_0 c \varepsilon_0}{2} |A_i|^2 \qquad i = 1, 2, 3 \tag{7}$$

As mentioned above, nonlinear optical indexes of the sample are essential parameters to adjust the hysteretic loop. In Eq. (5) there are two critical term; $n_2 \frac{\omega}{c} I_2 l$ and $\beta I_2 l$. If the first term dominates, the process is called dispersive bistability and if the second one dominates, it is called absorptive bistability [13]. In dispersive bistability, the nonlinear term leads to a periodic repetition of the generic S-shape deviations with a separation corresponding to $\delta = \frac{\lambda_0}{n_2 l}$ [14,17].

3. Results and discussions

A 16 μg/ml colloidal solution containing Au Nps in water was used in these experiments (the volume fraction is 8.3×10^{-7}) (TEM image in Fig. 2). Using dynamic light scattering (DLS), the size distribution of the particles has been obtained (Fig. 3). The average

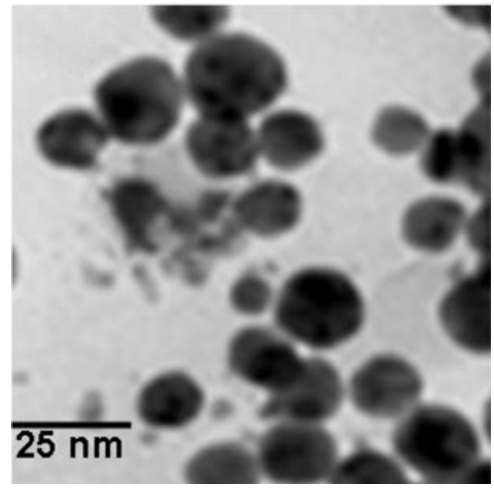

Fig. 2. TEM image of Au nanoparticles.

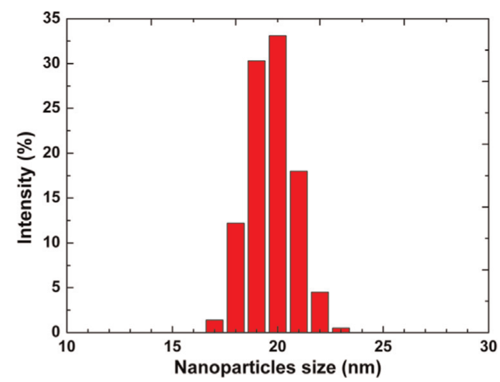

Fig. 3. Size distribution of the particles.

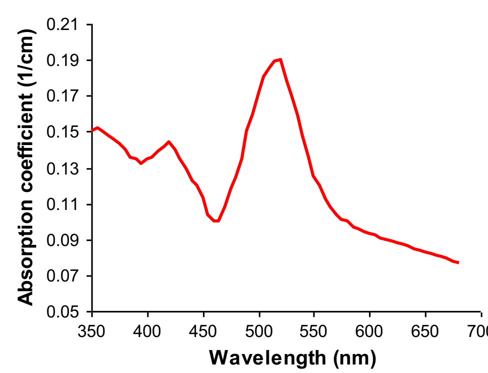

Fig. 4. Absorption spectrum of Au nano-colloid.

particle size is about 20 nm (standard deviation of SD+3.6 nm) and more than 98% of the particles are in the range of 18–22 nm.

The UV–visible absorption spectrum of the nanocolloid was shown in Fig. 4. The plasmon resonance peak could be observed at 520 nm.

First, obtaining nonlinear refractive index, close aperture z-scan method was utilized [18,19]. He–Ne laser and also Nd-YAG laser were used with the same spot size and incident power. A 1 mm length quartz cell containing the nanocolloid is irradiated with lasers beams that were focused with a converging lens. The waist of the beams at the focus ($z=0$) was 47 μm. The Rayleigh range of the He–Ne laser is 10.95 mm and for Nd-YAG laser is 13.04 mm. The distance between the focus and the aperture was 100 cm and the aperture transition was $S=0.1$. Fig. 5 depicts experimental and fitted theoretical curves for He–Ne laser. The assessed values have